RSC Advances

ROYAL SOCIETY OF CHEMISTRY

www.rsc.org/advances

Probing the origin of opposite ion-pair binding behavior for two new calix[4]pyrrole bis-phosphonate receptors

Teng Wang[a *], Jingjing Liu[b], Dongsheng Zhang[c], Hongwei Sun[d]

[a] *College of Chemical Engineering, Taishan Medical University, Taian, 271016, P.R. China.*
E-mail: wangteng@mail.nankai.edu.cn

[b] *College of Chemistry and Chemical Engineering, Taishan University, Taian, 271021, P.R. China.*

[c] *College of Radiation, Taishan Medical University, Taian, 271016, P.R. China.*

[d] *College of Chemistry, Nankai University, Tianjin, 300071, P.R. China.*

Abstract A new family of aryl-extended calix[4]pyrroles with two phoshonate groups can act as ion-pair receptors for guests alkylammonium/phosphonium chloride salts, and the ion-pair binding mode and binding affinity of these hosts are different. In the present contribution, the origin of opposite ion-pair binding behavior for two typical hosts ii and oo towards primary ammonium chloride salt and quaternary phosphonium chloride salt was investigated using quantum mechanics (QM) calculations and new nonconvalent weak interaction analysis method. Two types of arrangements – separated and contact – were taken into account for each complex. The binding energy suggests that contact and separated arrangements is the favorable binding mode for receptor ii and oo respectively. Furthermore, the primary alkylammonium chloride salt binds stronger to ii than to oo, while quaternary phosphonium chloride salt binds stronger to oo than to ii, in agreement with the experiment. Moreover, geometry, charge transfer based on natural bond orbital (NBO) and nonconvalent weak interactions analysis suggest that the hydrogen bonding and cation–π interactions play the critical role in ion-pair recognition of ii and oo respectively due to the different orientation of the P=O groups. This work further unveils the mechanism of ion-pair recognition by new calix[4]pyrrole bis-phosphonate receptors, while opening exciting perspectives for the design of stronger and more efficient calix[4]pyrrole-based ion-pair receptors.

Introduction

Ion-pair recognition is a fast growing research field in supramolecular chemistry.[1-6] In comparison with monotopic or single ion receptors that are designed to bind a cation or an anion alone, ditopic or ion-pair receptors with two disparate binding sites can simultaneously bind both cationic and anionic guest species. They have advantages in terms of substrate affinity and selectivity over monotopic receptors. Therefore, ion-pair receptors have potential use in salt solubilization,[7-9] ion extraction,[10-16] trans-membrane ion transport,[17-22] ion sensing,[23-27] and as logic gates.[28-30]

Calix[4]pyrroles such as *meso*-octamethylcalix[4]pyrrole (Fig. 1A) are macrocyclic molecules consisting of four pyrrole rings linked *via* sp^3 hybridized carbon atoms in the 2- and 5- positions. They have received significant attention recently due to their ability to bind anions and ion-pair salts.[4,6,31-34] Calix[4]pyrrole is generally conformationally flexible and has four typical conformations.[31,35,36] It adopts a 1,3-alternate conformation (Fig. 1B) in the absence of a bound anion. On the other hand, with the addition of anionic guests, it adopts the cone conformation (Fig. 1C and Fig. 1D). Then, in cone conformation, the calix[4]pyrrole provides an electron-rich aromatic cavity that serves as a receptor for cation. In addition, it can mainly bind cations and anions in two different modes, defined as close-contact (contact for short, Fig. 1C) and ion-separated (separated for short, Fig. 1D), respectively. In contact arrangement, the anion and cation are held in close proximity. While in separated arrangement, they are bound relatively far from one another.

Considerable effort was devoted to developing calix[4]pyrrole and its derivatives as ion-pair receptors.[22,24,26,37,38] Recently, Dalcanale and Ballester *et al.*[39] have reported a new family of aryl-extended calix[4]pyrroles (Fig. 2A) with two phoshonate groups. According to the relative spatial orientation of the P=O groups with respect to the aromatic cavity, they were named as ii (Fig. 2B), io, and oo (Fig. 2C) respectively. They can act as ion-pair receptors for alkylammonium/phosphonium (primary and quaternary) chloride salts in dichloromethane (DCM) solution and in the

solid state. The ion-pair binding mode and binding affinity are strongly modulated by the spatial orientation of the P=O groups. For the ii host, contact arrangement is the favorable binding mode and it binds primary alkylammonium chloride salt most tightly. On the contrary, for the oo host, separated arrangement is the favorable binding mode and it forms the most stable complexes with quaternary alkylphosphonium chloride salt.

Most recently, to explore the mechanism of ion-pair recognition by these new receptors, the ion-pair binding mode and binding affinity of the ii host towards quaternary alkylphosphonium chloride salt (tetramethylphosphonium chloride TMPCl, Fig. 2D) and primary alkylammonium chloride salt (ethylammonium chloride EAMCl, Fig. 2E) had been studied using quantum mechanics (QM) calculations.[40] We found that contact arrangement was the favorable binding mode for ii both in the gas-phase and in solution, in agreement with the experiment. Moreover, we also predicted that it preferred to bind primary ammonium chloride salt rather than quaternary phosphonium chloride salt. Furthermore, the main driving force responsible for the ion-pair recognition of ii had been revealed and hydrogen bonding interactions played the dominant role in this process.

However, as only ii host was considered to study ion-pair recognition in our previous work, the reason why there are differences in ion-pair binding behavior among these receptors is also not clear. In addition, traditional density functional theory (DFT) B3LYP method[41-43] was employed in previous paper and it may give inaccurate results in describing noncovalent interactions.

In the present work, QM calculations have been performed to study the origin of opposite ion-pair binding behavior including binding mode and binding affinity for two new calix[4]pyrrole bis-phosphonate receptors ii and oo both in the gas-phase and in DCM solution. To obtain more accurate noncovalent interactions, the new ωB97X-D[44,45] DFT-functional with dispersion corrections was employed. Thus, the ii host and its complexes investigated in our previous work were recalculated using this method. The ion-pair complexes of ii and oo were constructed and fully optimized. The geometrical feature, the binding affinity, and the charge transfer have been

discussed in detail. Moreover, the type and strength of nonconvalent weak interactions have been explored to unravel the mechanism responsible for the different ion-pair binding behavior of these two receptors.

Methods

The initial geometry of the hosts were taken from the published crystal structure,[39] and then the chloride anion and guest cations were introduced to build host:Cl^- and host:Cl^-:cation complexes. Two types of arrangements – contact and separated were considered for each guest cation. The geometry of the complexes was fully optimized in the gas-phase using DFT at the ωB97X-D/6-31G* level. The harmonic vibrational frequencies were also calculated at the same level of theory in order to confirm whether the obtained geometries corresponded to the energetic minima. Only a few very small imaginary frequencies (less than $50i$ cm^{-1}) were found for individual structures. This is because the numerical integration procedures used in DFT methods have significant limitations.[46] Thus, these low magnitude imaginary vibrational frequencies should imply that there is a genuine minimum of energy identical to or very close to the stationary point, and we do not follow the imaginary eigenvector in search of another minimum.

To evaluate the binding energy in ion-pair recognition, the complexation reaction steps was designed, as depicted in Fig. 3. The E^1_{deform} and E^2_{deform} are geometric deformation energy in binding chloride anion and cation respectively. The $E^1_{\text{interaction}}$ and $E^2_{\text{interaction}}$ are interaction energy between chloride anion and host and between cation and host:Cl^- complex respectively. Thus, the chloride anion binding energy E^1_{binding} and the cation binding energy E^2_{binding}, can be computed from the equation as follows respectively:

$$E^1_{\text{binding}} = E^1_{\text{deform}} + E^1_{\text{interaction}} \quad (1)$$

$$E^2_{\text{binding}} = E^2_{\text{deform}} + E^2_{\text{interaction}} \quad (2)$$

Therefore, the sum of E^{1}_{binding} and E^{2}_{binding} yields the total ion-pair binding energy E_{binding}. On the basis of optimized structures, the ωB97X-D method with 6-31++g** basis set was employed to calculate the binding energy. Moreover, the basis sets superposition error (BSSE) correction was taken into account to obtain an accurate interaction energy by using the counterpoise correction method.[47]

Based on the optimized structures in the gas-phase, the self-consistent reaction field (SCRF) method was chosen to model the DCM solvent environment to study solvation effects. In the SCRF calculations, Tomasi's polarized continuum model (PCM)[48] was used to calculate the binding energy using ωB97X-D method with 6-31++g** basis set.

To investigate the charge transfer in ion-pair recognition, the natural bond orbital (NBO)[49] analysis was implemented for the optimized structures by using the ωB97X-D method with 6-31++g** basis set.

To analyze and visualize the nonconvalent weak interactions between the host and guest, the electron density ($\rho(r)$) function, sign($\lambda_2(r)$)$\rho(r)$ function (sign($\lambda_2(r)$) means the sign of the second largest eigenvalue of electron density Hessian matrix at position r), and the reduced density gradient (RDG, $RDG(r)=\frac{1}{2\left(3\pi^2\right)^{1/3}}\frac{|\nabla\rho(r)|}{\rho(r)^{4/3}}$) function were calculated respectively. According to Yang's method,[50] noncovalent weak interactions are highly nonlocal and manifest in real space as low-gradient isosurfaces with low densities. The sign($\lambda_2(r)$) is used to give the type of interaction, and its strength can be derived from the density on the weak interaction surface. On the basis of optimized structures, utilizing different colors to represent sign($\lambda_2(r)$)$\rho(r)$ function value and map them onto RDG isosurfaces by Multiwfn 3.0[51] and VMD 1.9,[52] the type and the strength of weak interaction can be revealed visually.

All calculations were performed using the Gaussian 09 program.[53]

Results and Discussions

Geometry

The optimized structures of ii and ii complexes are shown in Fig. S1 (in the supplementary information), and the geometrical parameters are reported in Table S1 (in the supplementary information). First of all, the symmetry of the corresponding molecules optimized by ωB97X-D method are the same with those by B3LYP method as used in our previous work. Second, quantitatively very similar geometrical parameters including the amount and strength of hydrogen bonds are obtained from the two different methods. Therefore, the structural features calculated from the two methods are basically similar.

For oo and oo complexes, the optimized structures are represented in Fig. 4 and Fig. 5, and the corresponding structural data are gathered in Table 1. As shown in Fig. 4, the calix[4]pyrrole fragment transforms from a 1,3-alternate conformation in the free host to a cone conformation when binding chloride anion through N–H···Cl hydrogen bonds. In addition, the distances P1···P2 and O1···O2 are shorter in oo–Cl than that in oo, showing that the benzene rings are induced to come close to the chloride anion through anion–π interactions. These interactions can be confirmed in the following weak interaction analysis.

For contact arrangement oo–TMPCl–1, two weak C–H···O hydrogen bonds are formed between phosphonate groups and methyl groups. Because the phosphonate groups directed outwardly, the TMP cation forms hydrogen bonds with oxygen atoms in P–O single bonds while it forms hydrogen bonds with oxygen atoms in P=O double bonds in ii–TMPCl–1a and ii–TMPCl–1b. Moreover, the O···H distances and C–H···O angles are longer and smaller in oo–TMPCl–1 than that in ii–TMPCl–1a (both are 2.09 Å and 156.14°) and ii–TMPCl–1b (both are 2.17 Å and 134.38°) respectively, suggesting that the C–H···O hydrogen bonds in the former are weaker than that in the latter. For separated arrangement oo–TMPCl–2, no hydrogen bonds can be found between host and TMP cation.

For contact arrangement oo–EAMCl–1, three hydrogen bonds are established,

viz. N5–H5···Cl, N5–H6···O3, and N5–H7···O3, and these hydrogen bonds are relatively weak from the geometric viewpoint. Hydrogen bond N5–H5···Cl is stronger than hydrogen bonds N5–H6···O3 and N5–H7···O3. As the phosphonate groups are pointing outwardly, the EAM cation can only form hydrogen bonds with one phosphonate group while it forms hydrogen bonds with two phosphonate groups in ii–EAMCl–1. In addition, the O···H distances and N–H···O angles are longer and smaller in oo–EAMCl–1 than that in ii–EAMCl–1 (both are 1.88 Å and 143.72°) respectively, suggesting that the N–H···O hydrogen bonds in the former are weaker than that in the latter. Although the N–H···Cl hydrogen bond in oo–EAMCl–1 is slightly stronger than that in ii–EAMCl–1 (the H···Cl distance and N–H···Cl angle are 2.08 Å and 147.13° respectively), the total hydrogen bonding interactions in the former are weaker than that in the latter. For separated arrangement oo–EAMCl–2, there are also three hydrogen bonds are formed, *viz.* N5–H5···N4, N5–H6···N1, and N5–H7···N2. Furthermore, the distance H7···N2 is the shortest and the angle ∠N5–H7···N2 is the largest among the three hydrogen bonds, indicating that hydrogen bond N5–H7···N2 is stronger than hydrogen bonds N5–H5···N4 and N5–H6···N1.

Weak interaction

To investigate the weak interaction visually, the gradient isosurfaces of RDG for oo host and its complexes are delineated in Fig. 6 and Fig. 7. The surfaces are colored on a blue-green-red scale according to values of sign($\lambda_2(r)$)$\rho(r)$ over the range from -0.04 to 0.02 au. Blue indicates strong attraction, red indicates strong repulsion, and green indicates weak attractive interactions.

Similar to the ii host, there is steric repulsion (orange regions of the isosurface) between each pyrrole ring and its neighboring benzene rings and pyrrole rings in oo host (Fig. 6A) and that is the reason for energy barrier of conformational transition from 1,3-alternate to cone conformation. For oo–Cl complex (Fig. 6B), light blue regions of the isosurface can be clearly detected and these indicate N–H···Cl hydrogen bonding interactions. In addition, there are green regions between the

chloride anion and four benzene rings and can be identified as anion–π interactions.

For oo–TMPCl–1 (Fig. 7A), two weak C–H···O hydrogen bonds between methyls groups of TMP and phosphonate groups of oo can be found. Moreover, there are green areas between methyls groups and benzene rings, suggesting that there are cation–π interactions between TMP and oo. However, these green areas are very small and showing that the cation–π interactions are weak. In addition, van der Waals interactions between TMP and chloride anion can also be revealed. For oo–TMPCl–2 (Fig. 7B), the strong cation–π interactions between TMP and pyrrole rings of oo can be detected by large green areas. Furthermore, the charge–charge interactions between cations and anions for separated arrangement are stronger than those for contact arrangement according to the following NBO analysis. Although the charge–charge interactions are strong, these interactions cannot be displayed in gradient isosurfaces because this gradient isosurface is extremely small. Additionally, due to the large distance between TMP cation and chloride anion, the van der Waals interactions between them are very weak.

For oo–EAMCl–1 (Fig. 7C), N–H···O and N–H···Cl hydrogen bonds between EAM and oo can be identified. Among them, N–H···Cl hydrogen bond is strongest and can be located by blue area, in agreement with the geometry analysis above. In addition, there are weak cation–π and van der Waals interactions between EAM and benzene rings and between EAM and chloride anion respectively. For oo–EAMCl–2 (Fig. 7D), three N–H···N hydrogen bonds can be detected, and hydrogen bond N5–H7···N2 is stronger than hydrogen bonds N5–H5···N4 and N5–H6···N1, in agreement with the geometry analysis above. Moreover, there are large green areas between EAM and pyrrole rings, and they can be identified as strong cation–π interactions. In addition, the charge–charge interactions between cations and anions for separated arrangement are still stronger than those for contact arrangement and also cannot be displayed. The van der Waals interactions between EAM cation and chloride anion are also weak due to the large distance.

Charge transfer

To study the charge transfer in ion-pair recognition, charges of ions and hosts in oo complexes based on NBO analysis is reported in Table 2. For the ion-pair complexes of ii, the behavior of charge transfer is basically the same with that of B3LYP results (see Table S2).

For oo–Cl, electron transfer from chloride anion to the oo host through the N–H···Cl hydrogen bonding interactions. For oo–TMPCl–1, the charges of oo and chloride anion are less and more negative than that in oo–Cl respectively. The electron transfer from oo to the TMP through C–H···O hydrogen bonding interactions when binding this cation. On the other hand, the hydrogen bonds bring benzene rings of oo closer, and then some electron transfer from benzene rings of oo to the chloride anion due to the enhanced anion–π interactions. For oo–TMPCl–2, the negative charges of oo and chloride anion are both reduced compared to that in oo–Cl, indicating that the electron transfer from oo and chloride anion to TMP cation when binding it. Moreover, this charge transfer is just carried out by direct or indirect cation–π interactions. The electron transfer from oo to TMP through direct cation–π interactions. On the other hand, the electron of chloride anion transfer to the oo through N–H···Cl hydrogen bonding interactions, and then these electron transfer from oo that can be taken as the media of charge transfer to TMP through cation–π interactions. For oo–EAMCl–1, the electron transfer from oo and chloride anion to EAM cation through N–H···O and N–H···Cl hydrogen bonding interactions respectively. For oo–EAMCl–2, the electron transfer from oo to EAM cation through N–H···N hydrogen bonding and cation–π interactions, and the electron transfer from chloride anion to EAM cation through media oo.

The charge transfer comes from hydrogen bonding and cation–π interactions when binding cations, and the hydrogen bonding interactions hold a high percentage in it. Thus the charge transfer can reflect the strength of hydrogen bonds. The cations accept more negative charge in contact arrangements oo–TMPCl–1 and oo–EAMCl–1 than that in separated arrangements oo–TMPCl–2 and oo–EAMCl–2 respectively. The results show that the hydrogen bonding interactions in contact arrangements are

stronger than that in separated arrangements. Furthermore, the change of charge for cation in primary alkylammonium chloride salt complexes is larger than that in quaternary phosphonium chloride salt complexes, suggesting that the hydrogen bonding interactions in the former are stronger than that in the latter.

In addition, the dipole moments of oo complexes are also given in Table 2. For the ion-pair complexes of oo, the dipole moments of separated arrangements complexes are much smaller than that of contact arrangements complexes. This means that the centers of positive and negative charge approach much closer to each other in the former than they are in the latter. Therefore, the charge–charge interactions between ion-pair in separated arrangements are much stronger than that in contact arrangements. Although the hydrogen bonding interactions in separated arrangements are weaker than contact arrangements for oo complexes, the strong cation–π and charge–charge interactions make the former arrangements more energetically favorable.

Binding energy

To study the binding affinity of receptor ii and oo towards ion-pairs TMPCl and EAMCl, the binding energy in the gas-phase were calculated, as shown in Table 3.

For receptor ii, contact arrangements ii–TMPCl–1a, ii–TMPCl–1b and ii–EAMCl–1 are more favorable than separated arrangements ii–TMPCl–2a, ii–TMPCl–2b and ii–EAMCl–2 respectively, in agreement with the the results of experiment and B3LYP method. Furthermore, although pairwise competitive binding experiments were not conclusive for rating the binding affinity of ii with respect to TMPCl and EAMCl, the computational results indicate that it prefers to bind primary ammonium chloride salt rather than quaternary phosphonium chloride salt, also in agreement with the results of B3LYP method. In addition, the binding energy calculated from ωB97X-D method are more favorable than that from B3LYP method for the corresponding complexation reaction step, and this is because the former with dispersion corrections can account for dispersion binding. Although the absolute binding energy calculated from the two methods are different, the relative binding

affinity are same. The similar case also can be found in the following liquid-phase calculation.

For receptor oo, the binding energy of separated arrangements oo–TMPCl–2 and oo–EAMCl–2 are *ca.* 7.6 kcal mol^{-1} and 12 kcal mol^{-1} lower than that of contact arrangements oo–TMPCl–1 and oo–EAMCl–1 respectively. It is suggested that separated arrangement is the favorable binding mode for receptor oo, in agreement with the experiment. The reason can be explained in the following way. For oo–TMPCl complexes, only two weak C–H···O hydrogen bonds are formed in contact arrangement, while there are strong cation–π interactions between cation and pyrrole rings in separated arrangement. For oo–EAMCl complexes, although the hydrogen bond strength of one N–H···Cl and two N–H···O in contact arrangement are stronger than that of three N–H···N in separated arrangement, the cation–π interactions make a favorable contribution to the binding energy for the latter. In addition, the charge–charge interactions between ion-pair in separated arrangements are much stronger than that in contact arrangements as mentioned in dipole moments analysis. Therefore, oo prefers to separated arrangement rather than contact arrangement.

For TMPCl, the calculated binding energy of ii are lower than that of oo for each favorable arrangement, showing that ii binds TMPCl more strongly than oo in the gas-phase. However, according to experimental results, the order of binding affinity for the receptors towards TMPCl is oo ≈ 4 ii in DCM solvent. To study the solvation effects, the binding energy of contact arrangement for ii and two arrangements for oo were calculated in the DCM solvent and presented in Table 4. The results show that oo binds TMPCl more strongly than ii in the DCM solvent, in agreement with the experimental results. Firstly, the binding energy of oo–Cl is lower than that of ii–Cl, indicating that the binding affinity of chloride anion to the oo is greater than that of it to ii. This can be ascribed to the orientation of the P=O groups. The two oxygen atoms of the P=O groups are pointing inwardly with respect to the deep cavity in ii and there will be repulsive electrostatic interactions between the inwardly directed oxygen atoms of ii and the chloride anion. While the two oxygen atoms of P=O groups in oo

directed outwardly and there are no repulsive electrostatic interactions between oxygen atoms and the chloride anion. Therefore, although the E^1_{deform} of oo–Cl is less favorable than that of ii–Cl, the $E^1_{\text{interaction}}$ of the former is *ca.* 3 kcal mol^{-1} lower than that of the latter. Then, the $E^2_{\text{interaction}}$ of oo–TMPCl–2 is *ca.* 2.5 kcal mol^{-1} lower than that of ii–TMPCl–1b, suggesting that oo–Cl binds TMP cation more strongly than ii–Cl. Although there are C–H···O hydrogen bonds between cation and phosphonate groups in ii–TMPCl–1b, they are very weak. While there are strong cation–π interactions between cation and pyrrole rings in oo–TMPCl–2. Therefore, oo binds TMPCl more strongly than ii and cation–π interactions play the dominant role in this process. In addition, the solvation effects have an important influence on the ion-pair recognition.

For EAMCl, the calculated binding energy of ii are lower than that of oo for each favorable arrangement both in the gas-phase and DCM solvent, showing that ii binds EAMCl more strongly than oo. This is in agreement with the experimental results. The main reason is that there are two strong N–H···O hydrogen bonds and one strong N–H···Cl hydrogen bond in ii–EAMCl–1, and there are only three weak N–H···N hydrogen bonds in oo–EAMCl–2. Although there are strong cation–π interactions between cation and pyrrole rings in oo–EAMCl–2, it is weaker than the strong hydrogen bonding interactions in ii–EAMCl–1. Thus, the different binding affinity for the receptors towards EAMCl can be mainly ascribed to the hydrogen bonding interactions.

In addition, the calculation results show that oo binds EAMCl more strongly than TMPCl both in the gas-phase and DCM solvent. For oo–EAMCl–2, the favorable arrangement of oo–EAMCl complex, there are N–H···N hydrogen bonds and cation–π interactions between cation and host. While there are only cation–π interactions in favorable arrangement of oo–TMPCl complex – oo–TMPCl–2. Therefore, it seems that oo prefers to bind EAMCl rather than TMPCl. However, it is in contradiction with the experimental findings. The reason for this might be that the cation–π interactions in oo–TMPCl–2 are stronger than hydrogen bonding and

cation–π interactions in oo–EAMCl–2, and our calculation method cannot reflect this phenomenon very well.

Conclusions

The origin of different ion-pair binding behavior for new calix[4]pyrrole bis-phosphonate receptors ii and oo has been explored by QM calculations. The calculated binding energy of the ion-pair recognition suggests that contact and separated arrangements are the favorable binding modes for receptor ii and oo respectively. Furthermore, the primary alkylammonium chloride salt EAMCl binds stronger to ii than to oo, while quaternary phosphonium chloride salt TMPCl binds stronger to oo than to ii, in agreement with the experiment. Moreover, the computational results show that ii prefers to bind EAMCl rather than TMPCl, despite the experiments cannot give the binding affinity of ii with respect to these two guests. In addition, the calculation results also suggest that oo binds EAMCl more strongly than TMPCl, however, in contradiction with the experiment. The ion-pair binding behavior for ii and oo can be summed in Table 5.

Hydrogen bonding and cation–π interactions play the critical role in ion-pair recognition of ii and oo respectively due to the different orientation of the P=O groups. Concretely, the hydrogen bonding interactions between ii and guests in contact arrangements are stronger than that in separated arrangements, and cation–π interactions between oo and guests in separated arrangements are stronger than that in contact arrangements. Moreover, the charge–charge interactions between cations and anions in oo complexes for separated arrangements are stronger than those for contact arrangements due to the smaller dipole moment. Therefore, ii and oo prefer to contact and separated arrangements respectively. The cation–π interactions between oo and TMPCl in separated arrangement are stronger than hydrogen bonding interactions between ii and TMPCl in contact arrangement, and the hydrogen bonding interactions between ii and EAMCl in contact arrangement are stronger than cation–π interactions between oo and EAMCl in separated arrangement. This is the reason for different ion-pair binding affinity for ii and oo. In addition, the hydrogen bonding interactions

between ii and EAMCl are stronger than that between ii and TMPCl, and the cation–π interactions between oo and TMPCl are stronger than that between oo and EAMCl. This may explain why ii and oo prefer to bind EAMCl and TMPCl respectively.

The main reason responsible for the different ion-pair binding mode and binding affinity for new calix[4]pyrrole bis-phosphonate receptors ii and oo has been revealed at the electronic level, providing valuable insights into the potential of these calix[4]pyrrole-based supramolecular systems to act as ion-pair receptors. To better understand the origin of different ion-pair binding behavior, further investigation on the ion-pair recognition of transition receptor io is still needed. Moreover, other computational methods such as molecular dynamics simulations combined with free-energy calculations that may give accurate results in binding affinity and describing solvation effects are also needed, which are beyond the scope of this study.

Acknowledgements

This study was supported by the Research Award Fund for Outstanding Middle-Aged and Young Scientists of Shandong Province, China (no. BS2013YY061), the Natural Sciences Foundation of Shandong Province, China (no. ZR2013BL014), the Taishan Medical University (no. 2012GCC07) and the Taishan University (no. Y-01-2014013).

Electronic Supplementary Information (ESI)

Fig. S1 Side and top views of optimized structures of the ii and ii complexes

Table S1 Selected bond distances and bond angles for optimized structures of the ii and ii complexes

Table S2 NBO charges of ions and hosts and dipole moments in ii complexes

References

1. G. J. Kirkovits, J. A. Shriver, P. A. Gale and J. L. Sessler, *J. Inclusion Phenom. Macrocyclic Chem.*, 2001, **41**, 69−75.
2. P. D. Beer and P. A. Gale, *Angew. Chem. Int. Ed.*, 2001, **40**, 486−516.
3. B. D. Smith in *Macrocyclic Chemistry: Current Trends and Future Perspectives*, ed. K. Gloe, Springer, Dordrecht, Netherlands, 2005, pp. 137–151.
4. S. K. Kim and J. L. Sessler, *Chem. Soc. Rev.*, 2010, **39**, 3784–3809.
5. A. J. McConnell and P. D. Beer, *Angew. Chem., Int. Ed.*, 2012, **51**, 5052–5061.
6. M. Wenzel, J. R. Hiscock and P. A. Gale, *Chem. Soc. Rev.*, 2012, **41**, 480–520.
7. P. R. A. Webber and P. D. Beer, *Dalton Trans.*, 2003, 2249–2252.
8. G. Reeske, G. Bradtmoller, M. Schurmann and K. Jurkschat, *Chem. Eur. J.*, 2007, **13**, 10239–10245.
9. S. K. Kim, D. E. Gross, D. G. Cho, V. M. Lynch and J. L. Sessler, *J. Org. Chem.*, 2011, **76**, 1005–1012.
10. M. J. Deetz, M. Shang and B. D. Smith, *J. Am. Chem. Soc.*, 2000, **122**, 6201–6207.
11. J. M. Mahoney, A. M. Beatty and B. D. Smith, *Inorg. Chem.*, 2004, **43**, 7617–7621.
12. M. P. Wintergerst, T. G. Levitskaia, B. A. Moyer, J. L. Sessler and L. H. Delmau, *J. Am. Chem. Soc.*, 2008, **130**, 4129–4139.
13. A. Aydogan, D. J. Coady, S. K. Kim, A. Akar, C. W. Bielawski, M. Marquez and J. L. Sessler, *Angew. Chem. Int. Ed.*, 2008, **47**, 9648–9652.
14. R. S. Forgan, J. E. Davidson, F. P. A. Fabbiani, S. G. Galbraith, D. K. Henderson, S. A. Moggach, S. Parsons, P. A. Tasker and F. J. White, *Dalton Trans.*, 2010, **39**, 1763–1770.
15. S. K. Kim, V. M. Lynch, N. J. Young, B. P. Hay, C. H. Lee, J. S. Kim, B. A. Moyer and J. L. Sessler, *J. Am. Chem. Soc.*, 2012, **134**, 20837−20843.
16. J. Romanski and P. Piatek, *J. Org. Chem.*, 2013, **78**, 4341−4347.
17. L. A. J. Chrisstoffels, F. de Jong, D. N. Reinhoudt, S. Sivelli, L. Gazzola, A. Casnati and R. Ungaro, *J. Am. Chem. Soc.*, 1999, **121**, 10142−10151.

18. J. M. Mahoney, G. U. Nawaratna, A. M. Beatty, P. J. Duggan and B. D. Smith, *Inorg. Chem.*, 2004, **43**, 5902−5907.

19. A. P. Davis, D. N. Sheppardb and B. D. Smith, *Chem. Soc. Rev.*, 2007, **36**, 348–357.

20. C. C. Tong, R. Quesada, J. L. Sessler and P. A. Gale, *Chem. Commun.*, 2008, 6321−6323.

21. P. A. Gale, *Acc. Chem. Res.*, 2011, **44**, 216–226.

22. I. W. Park, J. Yoo, B. Kim, S. Adhikari, S. K. Kim, Y. Yeon, C. J. E. Haynes, J. L. Sutton, C. C. Tong, V. M. Lynch, J. L. Sessler, P. A. Gale and C. H. Lee, *Chem. Eur. J.*, 2012, **18**, 2514–2523.

23. J. M. Mahoney, A. M. Beatty and B. D. Smith, *J. Am. Chem. Soc.*, 2001, **123**, 5847–5848.

24. S. K. Kim, J. L. Sessler, D. E. Gross, C. H. Lee, J. S. Kim, V. M. Lynch, L. H. Delmau and B. P. Hay, *J. Am. Chem. Soc.*, 2010, **132**, 5827–5836.

25. M. Alfonso, A. Espinosa, A. Tarraga and P. Molina, *Org. Lett.*, 2011, **13**, 2078–2081.

26. S. K. Kim, G. I. Vargas-Zuniga, B. P. Hay, N. J. Young, L. H. Delmau, C. Masselin, C. H. Lee, J. S. Kim, V. M. Lynch, B. A. Moyer and J. L. Sessler, *J. Am. Chem. Soc.*, 2012, **134**, 1782–1792.

27. S. K. Kim, J. M. Lim, T. Pradhan, H. S. Jung, V. M. Lynch, J. S. Kim, D. Kim and J. L. Sessler, *J. Am. Chem. Soc.*, 2014, **136**, 495−505.

28. H. Miyaji, S. R. Collinson, I. Prokes and J. H. R. Tucker, *Chem. Commun.*, 2003, 64–65.

29. J. K. Choi, K. No, E. H. Lee, S. G. Kwon, K. W. Kim and J. S. Kim, *Supramol. Chem.*, 2007, **19**, 283–286.

30. D. S. Kim, V. M. Lynch, J. S. Park and J. L. Sessler, *J. Am. Chem. Soc.*, 2013, **135**, 14889−14894.

31. P. A. Gale, J. L. Sessler and V. Kral, *Chem. Commun.*, 1998, 1–8.

32. P. A. Gale, P. Anzenbacher Jr and J. L. Sessler, *Coord. Chem. Rev.*, 2001, **222**, 57–102.

33. P. A. Gale, J. L. Sessler, V. Kral and V. Lynch, *J. Am. Chem. Soc.*, 1996, **118**, 5140–5141.

34. R. Custelcean, L. H. Delmau, B. A. Moyer, J. L. Sessler, W. S. Cho, D. Gross, G. W. Bates, S. J. Brooks, M. E. Light and P. A. Gale, *Angew. Chem., Int. Ed.*, 2005, **44**, 2537–2542.

35. W. P. van Hoorn and W. L. Jorgensen, *J. Org. Chem.*, 1999, **64**, 7439–7444.

36. Y. D. Wu, D. F. Wang and J. L. Sessler, *J. Org. Chem.*, 2001, **66**, 3739–3746.

37. J. L. Sessler, S. K. Kim, D. E. Gross, C. H. Lee, J. S. Kim and V. M. Lynch, *J. Am. Chem. Soc.*, 2008, **130**, 13162–13166.

38. I. W. Park, J. Yoo, S. Adhikari, J. S. Park, J. L. Sessler and C. H. Lee, *Chem. Eur. J.*, 2012, **18**, 15073–15078.

39. M. Ciardi, F. Tancini, G. Gil-Ramirez, E. C. Escudero Adan, C. Massera, E. Dalcanale and P. Ballester, *J. Am. Chem. Soc.*, 2012, **134**, 13121–13132.

40. T. Wang, J. J. Liu, H. W. Sun, L. Chen, J. Dong, L. P. Sun and Y. S. Bi, *RSC Adv.*, 2014, **4**, 1864–1873.

41. A. D. Becke, *J. Chem. Phys.*, 1993, **98**, 5648–5652.

42. C. Lee, W. Yang and R. G. Parr, *Phys. Rev. B: Condens. Matter Mater. Phys.*, 1988, **37**, 785–789.

43. G. A. Petersson and M. A. Al-Laham, *J. Chem. Phys.*, 1991, **94**, 6081–6090.

44. J. D. Chai and M. Head-Gordon, *J. Chem. Phys.*, 2008, **128**, 084106.

45. J. D. Chai and M. Head-Gordon, *Phys. Chem. Chem. Phys.*, 2008, **10**, 6615–6620.

46. B. N. Papas and H. F. Schaefer, *J. Mol. Struct. (Theochem.)*, 2006, **768**, 175–181.

47. S. F. Boys and F. Bernardi, *Mol. Phys.*, 1970, **19**, 553–566.

48. S. Miertus, E. Scrocco and J. Tomasi, *Chem. Phys.*, 1981, **55**, 117–129.

49. A. E. Reed, L. A. Curtiss and F. Weinhold, *Chem. Rev.*, 1988, **88**, 899–926.

50. E. R. Johnson, S. Keinan, P. Mori-Sanchez, J. Contreras-Garcia, A. J. Cohen and W. Yang, *J. Am. Chem. Soc.*, 2010, **132**, 6498–6506.

51. T. Lu and F. Chen, *J. Comput. Chem.*, 2012, **33**, 580–592.

52. W. Humphrey, A. Dalke and K. Schulten, *J. Mol. Graphics*, 1996, **14**, 33–38.

53. M. J. Frisch, G. W. Trucks, H. B. Schlegel, G. E. Scuseria, M. A. Robb, J. R.

Cheeseman, G. Scalmani, V. Barone, B. Mennucci, G. A. Petersson, H. Nakatsuji, M. Caricato, X. Li, H. P. Hratchian, A. F. Izmaylov, J. Bloino, G. Zheng, J. L. Sonnenberg, M. Hada, M. Ehara, K. Toyota, R. Fukuda, J. Hasegawa, M. Ishida, T. Nakajima, Y. Honda, O. Kitao, H. Nakai, T. Vreven, J. A. Montgomery, Jr., J. E. Peralta, F. Ogliaro, M. Bearpark, J. J. Heyd, E. Brothers, K. N. Kudin, V. N. Staroverov, T. Keith, R. Kobayashi, J. Normand, K. Raghavachari, A. Rendell, J. C. Burant, S. S. Iyengar, J. Tomasi, M. Cossi, N. Rega, J. M. Millam, M. Klene, J. E. Knox, J. B. Cross, V. Bakken, C. Adamo, J. Jaramillo, R. Gomperts, R. E. Stratmann, O. Yazyev, A. J. Austin, R. Cammi, C. Pomelli, J. W. Ochterski, R. L. Martin, K. Morokuma, V. G. Zakrzewski, G. A. Voth, P. Salvador, J. J. Dannenberg, S. Dapprich, A. D. Daniels, O. Farkas, J. B. Foresman, J. V. Ortiz, J. Cioslowski, and D. J. Fox. Gaussian 09 (Revision B.01), Gaussian, Inc., Wallingford CT, 2010.

Figure Captions

Fig. 1 Structure of *meso*-octamethylcalix[4]pyrrole. (A) Structural formula (B) 1,3-alternate conformation (C) close-contact binding mode (D) ion-separated binding mode.

Fig. 2 Calix[4]pyrrole bis-phosphonate hosts and alkylphosphonium/ammonium chloride salts. (A) Structural formula with selected atom labels (B) ii (C) oo (D) TMPCl (E) EAMCl.

Fig. 3 Complexation reaction steps used to evaluate the binding energy in ion-pair recognition. CP represents the ii or oo host.

Fig. 4 Side and top views of optimized structures of oo (A) and oo–Cl (B).

Fig. 5 Side and top views of optimized structures of the oo–TMPCl and oo–EAMCl. (A) oo–TMPCl–1 (B) oo–TMPCl–2 (C) oo–EAMCl–1 (D) oo–EAMCl–2.

Fig. 6 Side and top views of gradient isosurfaces (RDG = 0.5 au) for oo (A) and oo–Cl (B).

Fig. 7 Side and top views of gradient isosurfaces (RDG = 0.5 au) for (A) oo–TMPCl–1 (B) oo–TMPCl–2 (C) oo–EAMCl–1 (D) oo–EAMCl–2.

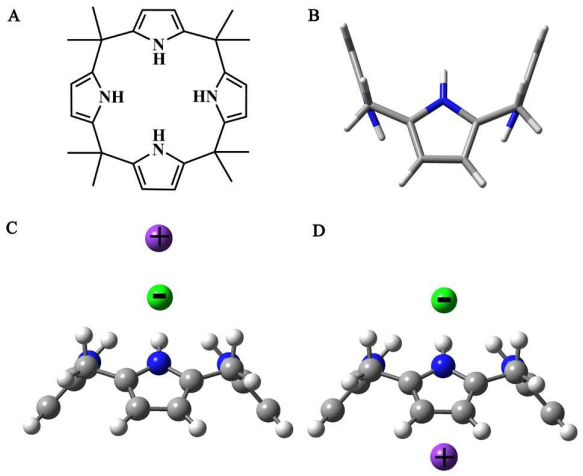

Fig. 1 Structure of *meso*-octamethylcalix[4]pyrrole. (A) Structural formula (B) 1,3-alternate conformation (C) close-contact binding mode (D) ion-separated binding mode.

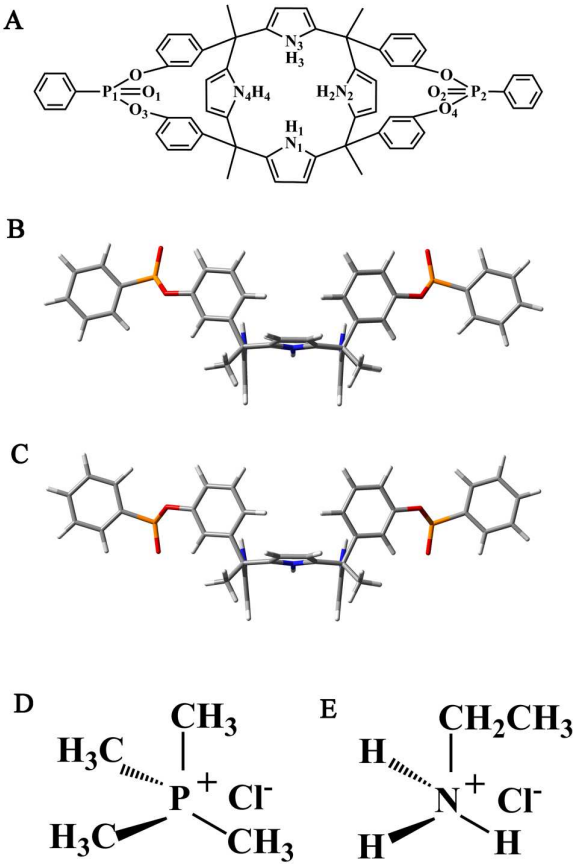

Fig. 2 Calix[4]pyrrole bis-phosphonate hosts and alkylphosphonium/ammonium chloride salts. (A) Structural formula with selected atom labels (B) ii (C) oo (D) TMPCl (E) EAMCl.

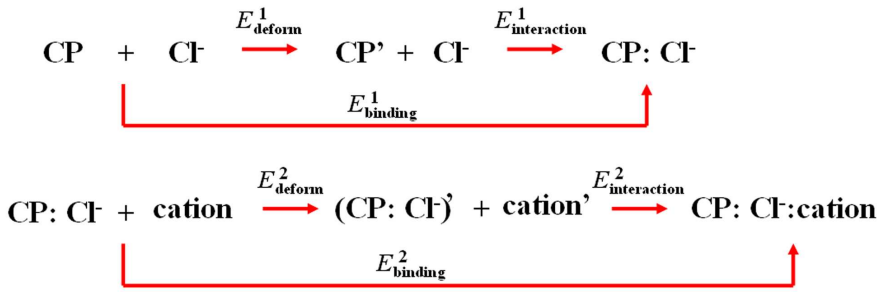

Fig. 3 Complexation reaction steps used to evaluate the binding energy in ion-pair recognition. CP represents the ii or oo host.

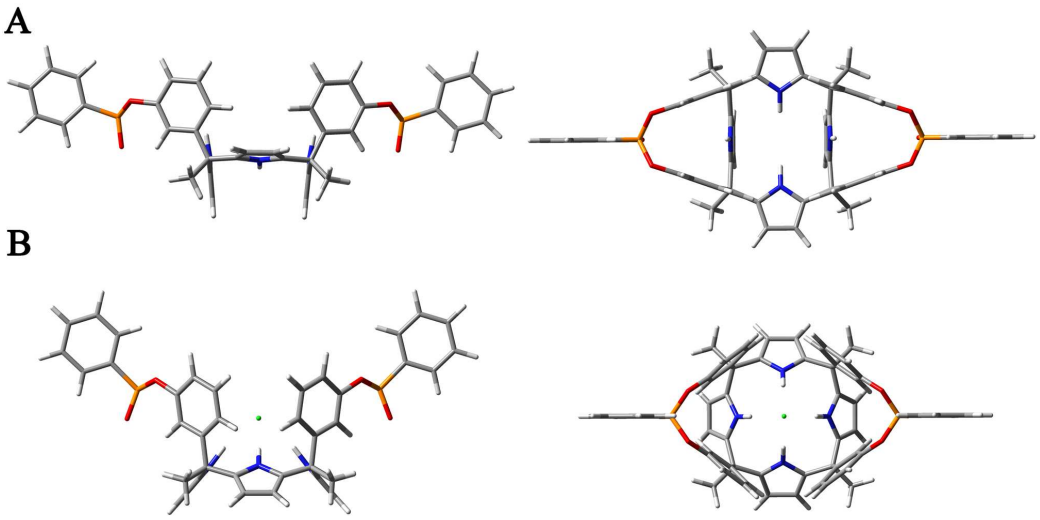

Fig. 4 Side and top views of optimized structures of oo (A) and oo–Cl (B).

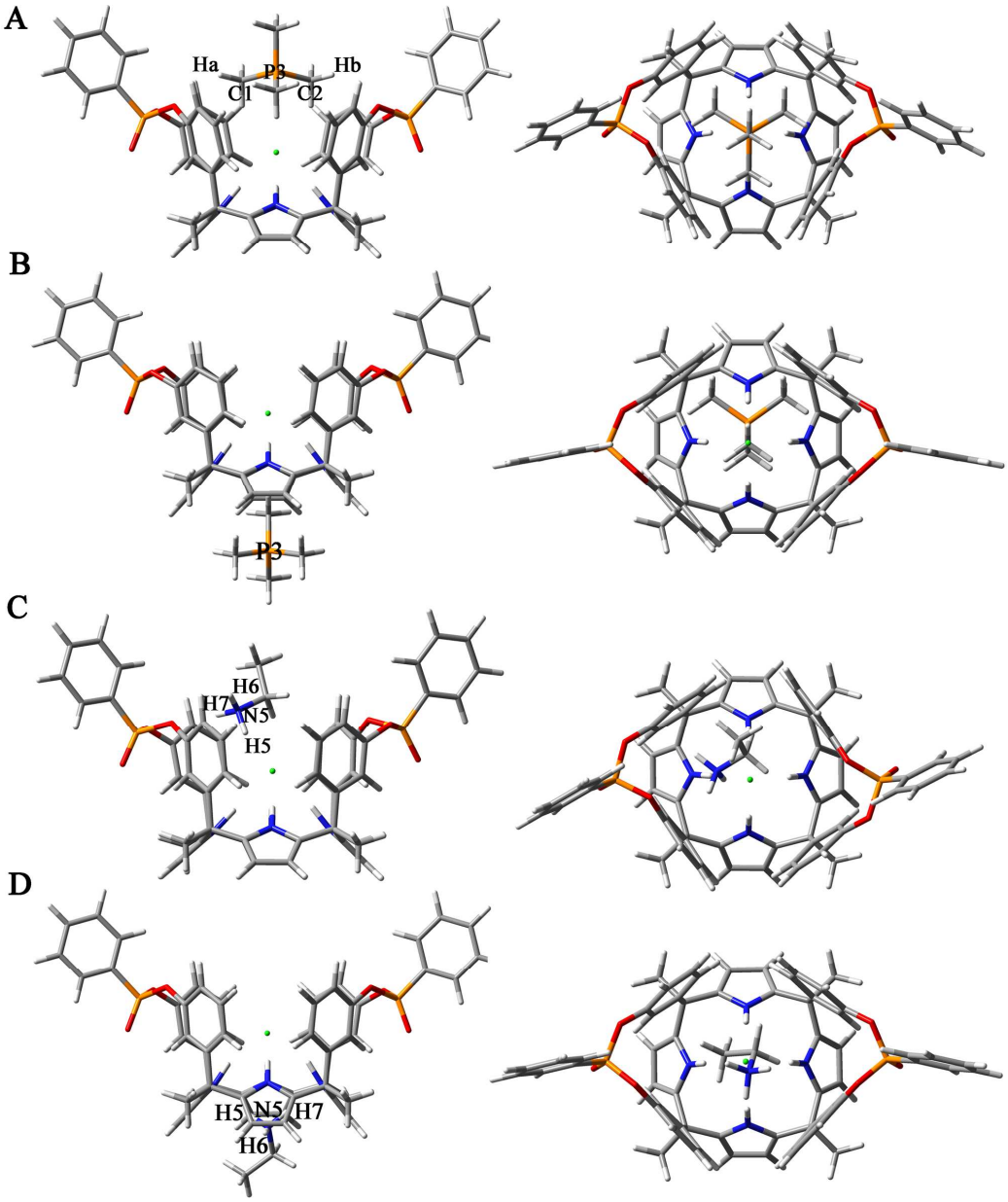

Fig. 5 Side and top views of optimized structures of the oo–TMPCl and oo–EAMCl. (A) oo–TMPCl–1 (B) oo–TMPCl–2 (C) oo–EAMCl–1 (D) oo–EAMCl–2.

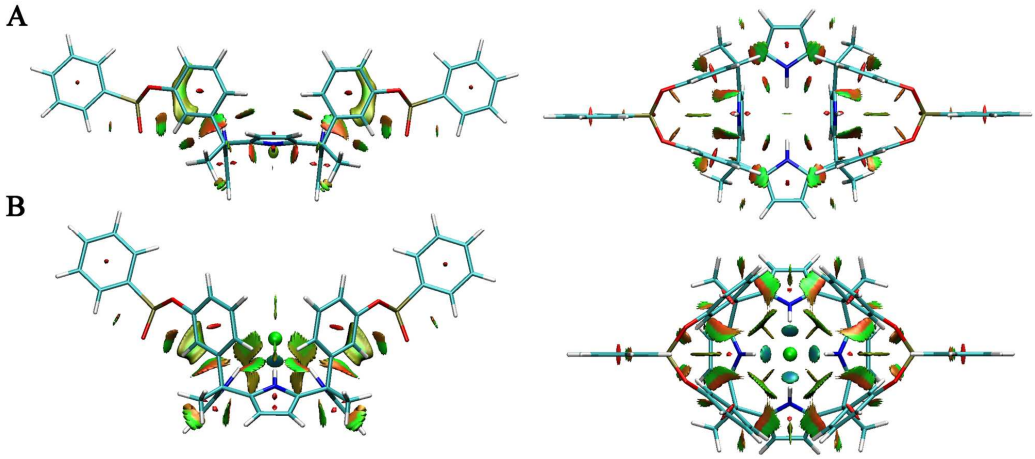

Fig. 6 Side and top views of gradient isosurfaces (RDG = 0.5 au) for oo (A) and oo–Cl (B).

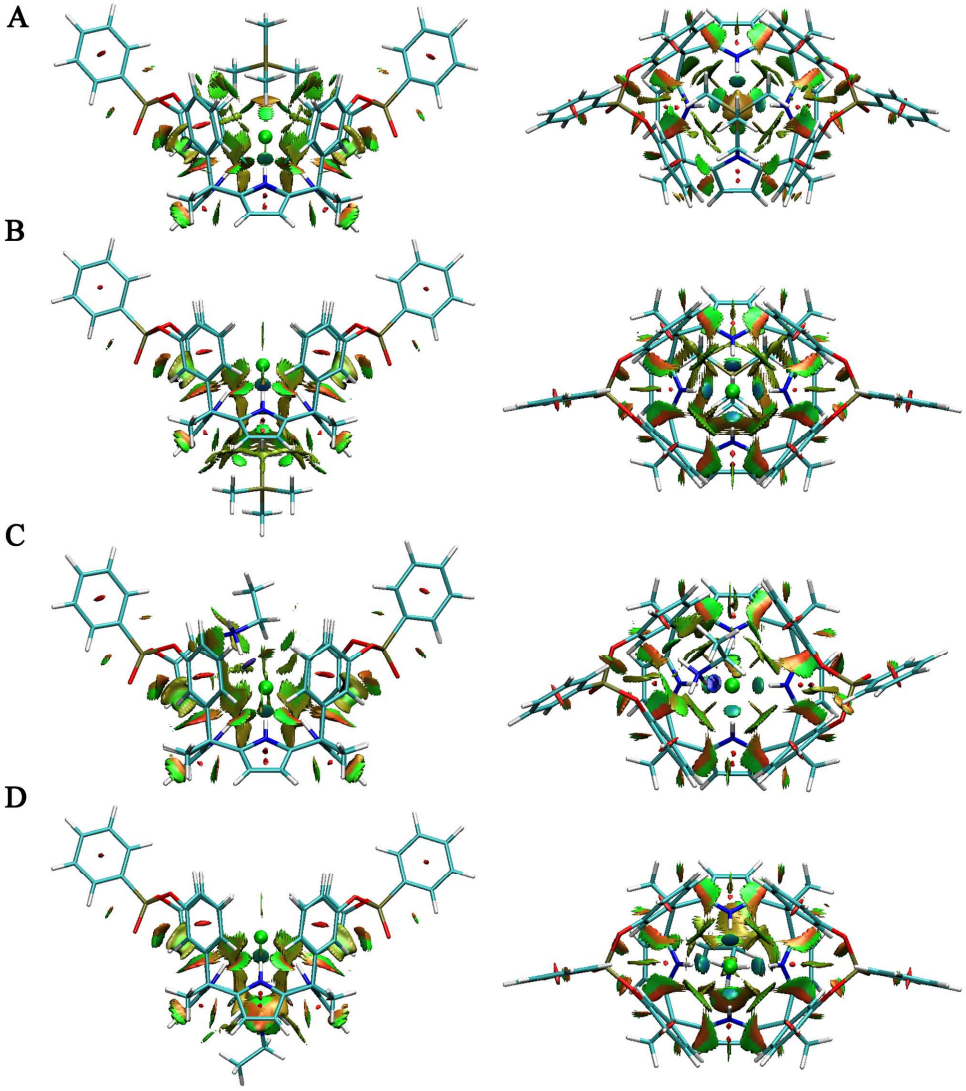

Fig. 7 Side and top views of gradient isosurfaces (RDG = 0.5 au) for
(A) oo–TMPCl–1 (B) oo–TMPCl–2 (C) oo–EAMCl–1 (D) oo–EAMCl–2.

Table 1 Selected bond distances (in Å) and bond angles (in degree) for optimized structures of the oo and oo complexes

parameter	oo	oo–Cl	oo–TMPCl–1	oo–TMPCl–2	oo–EAMCl–1	oo–EAMCl–2
symmetry	C_{2v}	C_{2v}	C_1	C_1	C_1	C_1
N1–H1	1.01	1.03	1.02	1.03	1.02	1.03
N2–H2	1.01	1.02	1.02	1.03	1.01	1.03
N3–H3	1.01	1.03	1.02	1.03	1.02	1.03
N4–H4	1.01	1.02	1.02	1.03	1.02	1.03
H1···Cl	–	2.22	2.27	2.16	2.24	2.24
H2···Cl	–	2.24	2.25	2.21	2.24	2.24
H3···Cl	–	2.22	2.23	2.23	2.29	2.18
H4···Cl	–	2.24	2.25	2.21	2.29	2.22
∠N1–H1···Cl	–	178.83	175.23	173.30	173.00	156.05
∠N2–H2···Cl	–	168.01	173.16	165.67	171.15	157.58
∠N3–H3···Cl	–	178.83	178.97	166.51	174.12	169.23
∠N4–H4···Cl	–	168.01	173.33	165.67	178.53	162.46
P3···Cl	–	–	3.51	6.09	–	–
P1···P2	14.03	11.61	11.32	11.45	10.87	11.32
O1···O2	13.65	12.64	12.36	12.44	12.11	12.32
O3···Ha	–	–	2.48	–	–	–
O4···Hb	–	–	2.50	–	–	–
∠C1–Ha···O3	–	–	134.29	–	–	–
∠C2–Hb···O4	–	–	132.82	–	–	–
N5···Cl	–	–	–	–	2.93	4.11
H5···Cl	–	–	–	–	1.94	–
O3···H6	–	–	–	–	2.68	–
O3···H7	–	–	–	–	2.60	–
∠N5–H5···Cl	–	–	–	–	155.33	–
∠N5–H6···O3	–	–	–	–	97.17	–
∠N5–H7···O3	–	–	–	–	101.30	–
H5···N4	–	–	–	–	–	2.02
H6···N1	–	–	–	–	–	2.55
H7···N2	–	–	–	–	–	1.98
∠N5–H5···N4	–	–	–	–	–	159.55
∠N5–H6···N1	–	–	–	–	–	105.05
∠N5–H7···N2	–	–	–	–	–	179.62

Table 2 NBO charges of ions and hosts and dipole moments (in Debye) in oo complexes

	oo–Cl	oo–TMPCl–1	oo–TMPCl–2	oo–EAMCl–1	oo–EAMCl–2
Cl	-0.766	-0.800	-0.740	-0.733	-0.749
TMP	–	0.951	0.958	–	–
EAM	–	–	–	0.858	0.919
oo	-0.234	-0.151	-0.218	-0.125	-0.170
dipole moment	9.519	18.664	8.244	16.161	1.351

Table 3 Calculated binding energy (in kcal mol^{-1}) in ion-pair recognition in the gas-phase

Complex	E^1_{deform}	$E^1_{interaction}$	$E^1_{interaction}$ (BSSE)	$E^1_{binding}$	$E^1_{binding}$ (BSSE)		
ii–Cl	10.70	-57.58	-56.70	-46.88	-46.00		
	E^2_{deform}	$E^2_{interaction}$	$E^2_{interaction}$ (BSSE)	$E^2_{binding}$	$E^2_{binding}$ (BSSE)	$E_{binding}$	$E_{binding}$ (BSSE)
ii–TMPCl–1a	4.65	-98.94	-96.50	-94.29	-91.85	-141.17	-137.85
ii–TMPCl–1b	4.17	-100.32	-97.79	-96.15	-93.62	-143.03	-139.62
ii–TMPCl–2a	2.02	-93.05	-90.88	-91.03	-88.86	-137.91	-134.86
ii–TMPCl–2b	1.79	-93.02	-90.88	-91.23	-89.09	-138.11	-135.09
ii–EAMCl–1	8.75	-133.98	-131.43	-125.23	-122.68	-172.11	-168.68
ii–EAMCl–2	4.39	-118.34	-116.23	-113.95	-111.84	-160.83	-157.84

Complex	E^1_{deform}	$E^1_{interaction}$	$E^1_{interaction}$ (BSSE)	$E^1_{binding}$	$E^1_{binding}$ (BSSE)		
oo–Cl	11.77	-57.83	-57.02	-46.06	-45.25		
	E^2_{deform}	$E^2_{interaction}$	$E^2_{interaction}$ (BSSE)	$E^2_{binding}$	$E^2_{binding}$ (BSSE)	$E_{binding}$	$E_{binding}$ (BSSE)
oo–TMPCl–1	3.57	-90.79	-88.36	-87.22	-84.79	-133.28	-130.04
oo–TMPCl–2	1.30	-95.91	-93.71	-94.61	-92.41	-140.67	-137.66
oo–EAMCl–1	2.15	-107.54	-105.90	-105.39	-103.75	-151.45	-149.00
oo–EAMCl–2	3.50	-121.35	-119.19	-117.85	-115.69	-163.91	-160.94

Table 4 Calculated binding energy (in kcal mol^{-1}) and experimental association constant value $K_{a,exp}$ (in M^{-1}) in ion-pair recognition in the DCM solvent

Complex	E^1_{deform}	$E^1_{interaction}$	$E^1_{binding}$	$K_{a,exp}$	
ii–Cl	5.60	-21.87	-16.27		
	E^2_{deform}	$E^2_{interaction}$	$E^2_{binding}$	$E_{binding}$	^{1}H NMR titration experiments	Isothermal titration calorimetry (ITC) experiments
ii–TMPCl–1a	0.70	-25.41	-24.71	-40.98		
ii–TMPCl–1b	-0.43	-25.51	-25.94	-42.21	$>10^4$	$2\pm0.5\times10^5$
ii–EAMCl–1	4.31	-43.52	-39.21	-55.48	$>10^4$	–
Complex	E^1_{deform}	$E^1_{interaction}$	$E^1_{binding}$			
oo–Cl	7.99	-24.66	-16.67			
	E^2_{deform}	$E^2_{interaction}$	$E^2_{binding}$	$E_{binding}$		
oo–TMPCl–1	0.67	-22.61	-21.94	-38.61	$>10^5$	$8\pm1\times10^5$
oo–TMPCl–2	-0.71	-28.02	-28.73	-45.40		
oo–EAMCl–1	0.50	-27.11	-26.61	-43.28	$2\pm1\times10^3$	–
oo–EAMCl–2	1.52	-35.47	-33.95	-50.62		

Table 5 Ion-pair binding behavior for ii and oo

	ii	oo
Critical Interactions	Hydrogen Bonding	Cation–π
Favorable Binding Modes	Contact	Separated
EAMCl Binding Affinity	ii > oo	
TMPCl Binding Affinity	oo > ii	
Favorable Binding Guests	EAMCl	TMPCl

Table of contents entry

Probing the origin of opposite ion-pair binding behavior for two new calix[4]pyrrole bis-phosphonate receptors

Teng Wang*, Jingjing Liu, Dongsheng Zhang, Hongwei Sun

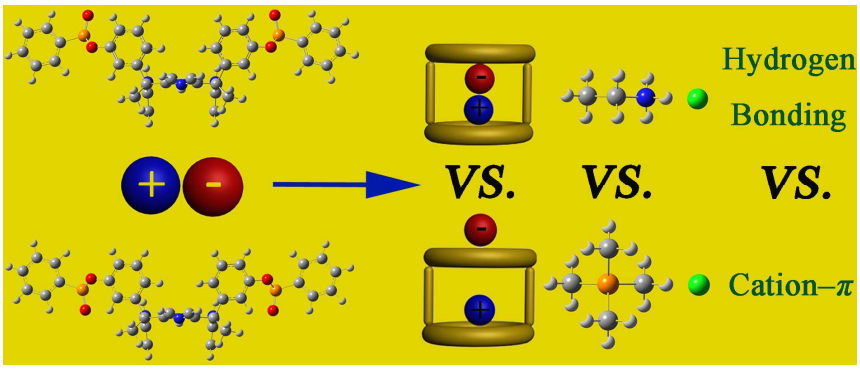

The origin of opposite ion-pair binding behavior for two new calix[4]pyrrole bis-phosphonate receptors has been explored.